Accepted Manuscript

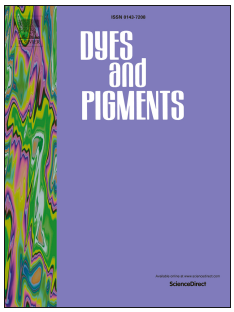

Near-infrared pH probes based on phenoxazinium connecting with nitrophenyl and pyridinyl groups

Wei-Jin Zhu, Jin-Yun Niu, Dan-Dan He, Ru Sun, Yu-Jie Xu, Jian-Feng Ge

PII: S0143-7208(17)31764-3

DOI: 10.1016/j.dyepig.2017.09.059

Reference: DYPI 6285

To appear in: *Dyes and Pigments*

Received Date: 17 August 2017

Revised Date: 23 September 2017

Accepted Date: 23 September 2017

Please cite this article as: Zhu W-J, Niu J-Y, He D-D, Sun R, Xu Y-J, Ge J-F, Near-infrared pH probes based on phenoxazinium connecting with nitrophenyl and pyridinyl groups, *Dyes and Pigments* (2017), doi: 10.1016/j.dyepig.2017.09.059.

Graphical abstract

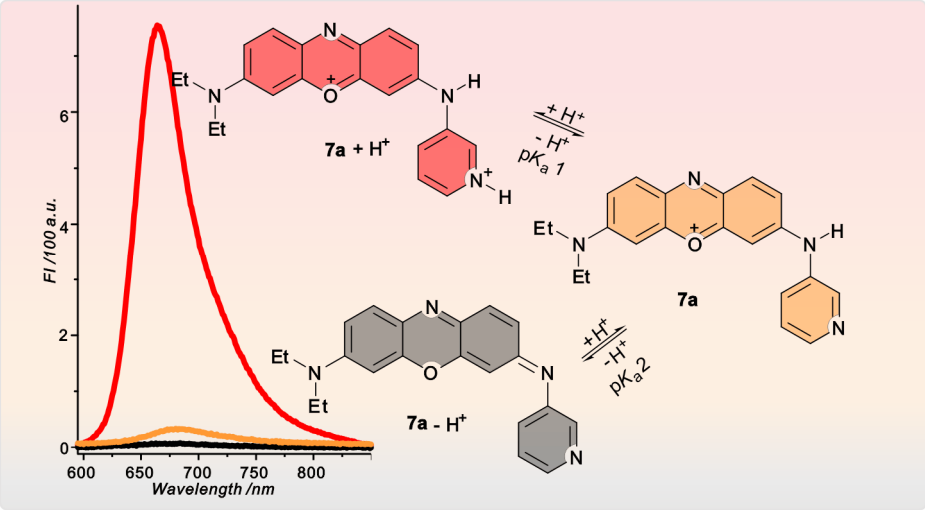

Near-infrared pH probes based on phenoxazinium connecting with nitrophenyl and pyridinyl groups

Wei-Jin Zhu,[‡a] Jin-Yun Niu,[‡b] Dan-Dan He,[a] Ru Sun,[a] Yu-Jie Xu,[*b] Jian-Feng Ge[*a,c]

[a].*College of Chemistry, Chemical Engineering and Material Science, Soochow University, 199 Ren'Ai Road, Suzhou 215123, China.*

[b].*Technology School of Radiation Medicine and Protection, Medical College of Soochow University, School for Radiological and Interdisciplinary Sciences (RAD-X), Soochow University, Suzhou 215123, China.*

[c].*Jiangsu Key Laboratory of Medical Optics, Suzhou Institute of Biomedical Engineering and Technology, Chinese Academy of Sciences, Suzhou 215163, China.*

[‡]These authors contributed equally.

Abstract: Three phenoxazinium compounds attached with *o*-nitrophenyl (**3a**), *m*-nitrophenyl (**3b**) and *p*-nitrophenyl (**3c**) groups were prepared, and the pH promoted emission spectra were used to evaluate the deprotonated-protonated equilibrium between phenoxazinium and phenoxazine. They showed nearly ON-OFF emission responses at 650−850 nm around pH 8.0−10.8, and the fluorescence related pK_as of **3a–c** were 8.7, 9.2, and 8.9, respectively. Two phenoxazinium compounds attached with pyridinyl groups (**7a–b**) were further prepared, the pH promoted emission spectra were influenced by both the deprotonated-protonated equilibrium between phenoxazinium and phenoxazine, and the equilibrium between pyridinyl group and pyridinumyl group. They exhibited more strong red and

[*]*Corresponding authors. Tel. & fax: +86 0512 6588 4717. E-mail addresses: dbnm@suda.edu.cn, ge_jianfeng@hotmail.com(J.-F. Ge).*

near-infrared emission at 600–850 nm, probe **7a** gave pK_a,1 = 3.71 and pK_a,2 = 9.68, and that of probe **7b** was 2.75. Moreover, the fluorescent imaging experiment indicated that probe **7a** was a lysosome biomarker for V79 and HeLa cells.

Keyword: phenoxazinium, equilibrium, Rosamine, near-infrared emission, lysosome biomarker.

1. Introduction

Fluorescent dyes play a vital role in the family of functional dyes and they are applied extensively in different fields of science and technology. pH is an important parameter in a broad range of applications in environment, industry and biological field. The study of pH fluorescent probes in life science,[1-3] clinical diagnosis[4] and immunological detection[5] has become hot topics.[6-10] Many pH sensors concerned in life science, food and beverage processing, soil examination, marine, and pharmaceutical research. Compared with normal pH indicators, fluorescent pH probes have attracted considerable attention because the fluorescent method can give more precise analysis results.[11, 12] In addition, due to minimum photo-damage to biological samples, deep tissue penetration, and minimum interference from background auto-fluorescence by biomolecules in the living systems, so fluorescent pH probes with near-infrared (NIR) emission is favorable and important for in vivo bioimaging.[13, 14]

The usual method in design of fluorescent pH probes is based on the nitrogen and oxygen related reaction, and the deprotonated and protonated processes of amino group or phenolic anion produce optical responses by intramolecular charge

transfer (ICT)[15] or photoinduced electron transfer (PET) mechanisms.[16, 17] Another method is the application of reaction based mechanisms, for example, the ring-opening reaction of the rhodamine,[18] cyanine based protonation of the free amine group,[19] etc. Based on the limited design methods, most reported pH probes work in neutral or subacidic conditions,[20-24] therefore, new pH responsive reaction is needed for wider pH detection.

Benzo[a]phenoxazine derivatives were reported as stable and biocompatibile compounds,[25, 26] the related probes can be easily redesigned to obtain the properties of NIR absorption and emission;[26] among them, benzo[a]phenoxazines with N-aromatic groups were reported as pH probes in subacidic and strong acidic conditions.[27] Phenoxazinium is another oxazine-type compound difference from benzo[a]phenoxazine,[28] the disclosure of the pH activable optical properties will benefit for both the inside view of phenoxazinium and pH probe application in chemical and biological fields.

2. Experimental

2.1. Materials and apparatus

All reagents and solvents (synthetic or analytical grade) were purchased from TCI Development Co., Ltd (Tokyo, Japan), Sinopharm Chemical Reagent Co., Ltd (Shanghai, China) and Energy Chemical Co., Ltd (Shanghai, China). Flash chromatography was performed with silica gel (300–400 mesh). ^{1}H-NMR and ^{13}C-NMR spectra were recorded on a Varian or Agilent spectrometer, solvent peaks were used as internal standards, which were underlined in supporting spectra. High

resolution mass spectra were recorded on a Finnigan MAT95 mass spectrometer (ESI^+). Melting points were determined on an X-4 microscope electron thermal apparatus (Taike, China).

UV-vis spectra were recorded on a Shimadzu UV-1800 spectrophotometer. Fluorescence emission spectra were recorded with a fused quartz cuvette (10 mm × 10 mm) on a Shimadzu RF-5301PC spectrometer with an R-928 photomultiplier at room temperature; the excitation and emission slit widths were all set at 5/5 or 3/5 nm. The pH values were measured with a Lei-Ci (pH-3C) digital pH meter (Shanghai, China) using a combined glass-calomel electrode. Cells were cultured in Roswell Park Memorial Instrument media (RPMI-1640). Fluorescence confocal images were recorded with Leica TCS SP5 II confocal laser scanning microscope.

2.2. Synthesis and characterization

*2.2.1. General method of preparation of **2a–c***

A mixture of 3-methoxyl-*N*-nitrophenylaniline (**1a–c**, 1.83 g, 7.5 mmol), concentrated HCl (30 mL) and CH_3CN (67.5 mL) was stirred in an ice bath. $NaNO_2$ (724.4 mg, 10.5 mmol) was slowly added to the mixture in small portions within 1 h, and the resulting mixture was stirred in ice bath for another 1 h. The solution was basified to pH ≈ 8−9 by the addition of K_2CO_3 powder, then it was extracted with CH_2Cl_2 (3 × 20.0 mL), the extract was dried over anhydrous magnesium sulfate and evaporated. The residue was purified by column chromatography (**2a**: eluting with 3:1(v/v) petroleum ether / ethyl acetate, **2b**: eluting with 5:1(v/v) CH_2Cl_2/ ethyl acetate, **2c**: eluting with 7:1(v/v) CH_2Cl_2/ ethyl acetate); the eluent was evaporated;

the residue was ultra-sonicated in small amount of Et_2O, and filtrated to give the compounds **2a–c**.

2.2.2. *3-Methoxy-N-(2-nitrophenyl)-4-nitrosoaniline (**2a**)*

Orange solid, 0.85 g, yield 41.3 %, mp 156.0 – 156.6 ^{o}C, ^{1}H NMR (400 MHz, $CDCl_3$) δ 9.43 (s, 1H, -N*H*), 8.24 (d, J = 8.5 Hz, 1H, Ar-*H*), 7.65 – 7.58 (m, 2H, 2×Ar-*H*), 7.11 (t, J = 7.7 Hz, 1H, Ar-*H*), 6.99 (s, 1H, Ar-*H*), 6.68 (d, J = 8.9 Hz, 1H, Ar-*H*), 6.51 (d, J = 8.6 Hz, 1H, Ar-*H*), 4.24 (s, 3H, -C*H*$_3$). ^{13}C NMR (101 MHz, $CDCl_3$) 164.3, 157.0, 150.1, 138.1, 137.6, 135.9, 127.3, 122.2, 120.1, 112.1, 110.4, 103.2, 56.9. HRMS-ESI$^+$: found m/z = 274.0811 (calcd for $[M + H^+]^+$, 274.0828).

2.2.3. *3-Methoxy-N-(3-nitrophenyl)-4-nitrosoaniline (**2b**)*

Yellow brown solid, 1.05 g, yield 51.3 %, mp 172.2 – 172.7 ^{o}C, ^{1}H NMR (400 MHz, DMSO-d_6) δ 10.02 (s, 1H, -N*H*), 8.06 – 7.66 (m, 4H, 4×Ar-*H*), 6.86 (s, 1H, Ar-*H*), 6.51 (d, J = 11.1 Hz, 2H, 2×Ar-*H*), 4.10 (s, 3H, -CH_3). ^{13}C NMR (101 MHz, DMSO-d_6) 165.0, 157.4, 154.2, 149.3, 141.5, 131.7, 127.7, 118.7, 115.8, 112.8, 107.7, 97.2, 56.8. HRMS-ESI$^+$: found m/z = 274.0822 (calcd for $[M + H^+]^+$, 274.0828).

2.2.4. *3-Methoxy-N-(4-nitrophenyl)-4-nitrosoaniline (**2c**)*

Orange solid, 0.90 g, yield 44.0 %, mp 173.9 – 174.5 ^{o}C, ^{1}H NMR (400 MHz, DMSO-d_6) δ 10.22 (s, 1H, -N*H*), 8.24 (d, J = 9.1 Hz, 2H, 2×Ar-*H*), 7.49 (d, J = 9.0 Hz, 2H, 2×Ar-*H*), 7.03 (s, 1H, Ar-*H*), 6.65 (d, J = 9.1 Hz, 1H, Ar-*H*), 6.47 (d, J = 9.1 Hz, 1H, Ar-*H*), 4.15 (s, 3H, -C*H*$_3$). ^{13}C NMR (101 MHz, DMSO-d_6) 163.4, 156.2, 151.6, 146.1, 141.0, 125.2, 118.5, 111.2, 107.9, 98.5, 55.8. HRMS-ESI$^+$: found m/z = 274.0822 (calcd for $[M + H^+]^+$, 274.0828).

2.2.5. *General method of preparation of* ***3a–c***

The mixture of 3-(diethylamino)phenol (363.3 mg, 2.2 mmol) and 90% *i*-PrOH (44 mL) was stirred at 70 ^{o}C in a 250 mL two-neck bottle filled with nitrogen atmosphere. A suspended solution with 3-methoxy-*N*-nitrophenyl-4-nitrosoaniline (**2a–c**, 600.8 mg, 2.2 mmol) and concentrated hydrochloric acid (183 μL, 2.2 mmol) in 90% *i*-PrOH (44 mL) was injected with syringe to the reaction in four portions during 45 min. The temperature rose to reflux. When about 45 mL volume of the solvent was distilled out, 45 mL of 90% *i*-PrOH was added to the reaction mixture; this procedure was repeated three times during 3–4 h. The dark solution was concentrated, the residue was purified by column silica gel chromatography eluting with $CHCl_3$/MeOH from 20:1 to 10:1 (v/v), and the eluent was evaporated, the residue was ultra-sonicated in small amount of Et_2O, the powder (**3a–c**) was obtained after filtration and vacuum drying.

2.2.6. *3-(Diethylamino)-7-((2-nitrophenyl)amino)phenoxazin-5-ium chloride (**3a**)*

Dark solid, 140.0 mg, yield 15.0 %, mp 128.5–130.5 ^{o}C. ^{1}H NMR (400 MHz, $CDCl_3$:CD_3OD=8:1(v/v)) δ 8.07 (d, J = 7.4 Hz, 1H, Ar-*H*), 7.64 – 7.03 (m, 6H, 6×Ar-*H*), 6.72 – 6.20 (m, 3H, 3×Ar-*H*), 6.03 (s, 1H, N*H*), 3.49 (br, 4H, 2×-CH_2), 1.25 (br, 6H, 2×-CH_3). ^{13}C NMR (75 MHz, TFA-*d*) 160.9, 155.2, 153.7, 152.4, 142.4, 139.4, 138.7, 136.5, 134.9, 133.3, 132.3, 129.5, 128.9, 125.5, 125.2, 123.2, 104.2, 101.4, 51.2, 14.1. HRMS-ESI^{+}: found m/z = 389.1608 (calcd for [M - Cl^{-}]$^{+}$, 389.1614).

2.2.7. *3-(Diethylamino)-7-((3-nitrophenyl)amino)phenoxazin-5-ium chloride (**3b**)*

Dark solid, 186.6 mg, yield 20.0 %, mp 117.0 – 119.0 ^{o}C. ^{1}H NMR (400 MHz,

DMSO-d_6) δ 7.93 (d, J = 7.7 Hz, 1H, Ar-*H*), 7.65 – 7.61 (m, 2H, 2×Ar-*H*), 7.40 (d, J = 8.9 Hz, 1H, Ar-*H*), 7.32 (d, J = 7.2 Hz, 1H, Ar-*H*), 7.18 (d, J = 9.7 Hz, 1H, Ar-*H*), 6.90 (s, 1H, Ar-*H*), 6.71 (d, J = 8.1 Hz, 1H, Ar-*H*), 6.43 (s, 1H, Ar-*H*), 6.12 (s, 1H, Ar-*H*), 3.44 (d, J = 6.7 Hz, 4H, 2×-CH_2), 1.12 (t, J = 6.8 Hz, 6H, 2×-CH_3). ^{13}C NMR (75 MHz, DMSO-d_6) δ 159.2, 151.7, 150.2, 148.8, 148.6, 148.0, 147.6, 145.7, 141.4, 131.8, 130.2, 130.0, 127.0, 125.0, 117.3, 114.3, 109.5, 95.3, 43.8, 11.9. HRMS-ESI$^+$: found m/z = 389.1608 (calcd for [M – Cl$^-$]$^+$, 389.1614).

2.2.8. *3-(Diethylamino)-7-((4-nitrophenyl)amino)phenoxazin-5-ium chloride (**3c**)*

Dark solid, 156.9 mg, yield 16.8 %, mp 151.2 – 153.2 ^{o}C. ^{1}H NMR (400 MHz, CD_3OD) δ 8.32 (d, J = 7.8 Hz, 2H, 2×Ar-*H*), 7.97 (d, J = 8.8 Hz, 1H, Ar-*H*), 7.88 (d, J = 9.6 Hz, 1H, Ar-*H*), 7.66 (d, J = 9.5 Hz, 1H, Ar-*H*), 7.56 (d, J = 7.7 Hz, 2H, 2×Ar-*H*), 7.48 (d, J = 8.7 Hz, 1H, Ar-*H*), 7.40 (s, 1H, Ar-*H*), 7.13 (s, 1H, Ar-*H*), 3.92 (s, 4H, 2×-CH_2), 1.43 (s, 6H, 2×-CH_3). ^{13}C NMR (101 MHz, TFA-*d*) δ 166.2, 165.7, 165.3, 164.9, 161.6, 157.0, 148.1, 147.9, 139.1, 135.3, 134.1, 132.8, 129.6, 126.0, 125.4, 123.9, 122.3, 119.4, 116.6, 113.9, 104.4, 102.6, 52.2, 15.1. HRMS-ESI$^+$: found m/z = 389.1608 (calcd for [M – Cl$^-$]$^+$, 389.1614).

2.2.9. *Synthesis of N-(3-methoxyphenyl)-N-methylpyridin-3-amine (**5b**)*

To a solution of **5a** (2.00 g, 10.00 mmol) and *t*-BuOK (2.24 g, 20.00 mmol) in *N, N*-dimethylformamide (DMF, 100.0 mL), iodomethane (1.2 mL, 20 mmol) was added. The resulting solution was stirred for 12 hours at room temperature. Then water (100 mL) was added, the solution was extracted with ethyl acetate (3 × 30 mL), and the organic layer was evaporated by evaporation. The residue was purified by column

chromatograph on silica gel eluting with dichloromethane, ethyl acetate and triethylamine (20:1:0.1, v/v/v) to afford product as white solid (1.40 g, 65.0%). ^{1}H NMR (400 MHz, $CDCl_3$) δ 8.44 (d, J = 2.3 Hz, 1H, Ar-*H*), 8.25 (d, J = 4.4 Hz, 1H, Ar-*H*), 7.36 (d, J = 8.9 Hz, 1H, Ar-*H*), 7.30 (t, J = 8.2 Hz, 1H, Ar-*H*), 7.24 (dd, J = 8.2, 4.6 Hz, 1H, Ar-*H*), 6.74 (d, J = 8.4 Hz, 1H, Ar-*H*), 6.70-6.68 (m, 2H, 2×Ar-*H*), 3.85 (s, 3H, -CH_3), 3.41 (s, 3H, -CH_3). ^{13}C NMR (151 MHz, $CDCl_3$) δ 160.8, 149.2, 145.0, 141.6, 141.5, 130.2, 125.8, 123.4, 114.0, 108.0, 107.6, 55.2, 40.0. HRMS (ESI^+): m/z = 215.1179 (calcd for $[M + H^+]^+$, 215.1184).

2.3.0. *Synthesis of N-(3-methoxy-4-nitrosophenyl)pyridin-3-amine (**6a**)*

To a solution of **5a** (100.1 mg, 0.50 mmol) and acetonitrile (3.0 mL) in an ice water bath, hydrochloric acid (3.0 mL) and water (450 μL) were added. After stirring for a while, sodium nitrite (48.6 mg, 0.70 mmol) was added slowly within 20 min. The resulting solution was stirred for further 1 hour at 0 ^{o}C. The solution was treated with potassium carbonate to pH ≈ 9, and then it was extracted with dichloromethane (3 × 30 mL). After evaporation, the residue was purified by column chromatograph on silica gel eluting with acetonitrile, ethyl acetate and triethylamine (3:1:0.1, v/v/v), to afford product as green solid, 90.2 mg, yield 78.7%, mp 151.0 – 152.0 ^{o}C. ^{1}H NMR (400 MHz, DMSO-d_6) δ 9.81 (s, 1H, N*H*), 8.57 (s, 1H, Ar-*H*), 8.38 (d, J = 4.6 Hz, 1H, Ar-*H*), 7.82 (d, J = 8.2 Hz, 1H, Ar-*H*), 7.47 – 7.44 (m, 1H, Ar-*H*), 6.74 (s, 1H, Ar-*H*), 6.50 – 6.44 (m, 2H, 2×Ar-*H*), 4.09 (s, 3H, -CH_3). ^{13}C NMR (75 MHz, DMSO-d_6) δ 165.0, 157.2, 155.0, 145.5, 143.9, 136.5, 129.3, 124.7, 112.8, 107.1, 95.9, 56.5. HRMS (ESI^+): m/z = 230.0910 (calcd for $[M + H^+]^+$, 230.0930).

2.3.1. *Synthesis of N-(3-methoxy-4-nitrosophenyl)-N-methylpyridin-3-amine (**6b**)*

To a solution of **5b** (256.0 mg, 1.20 mmol) and tetrahydrofuran (18.2 mL) in an ice water bath, hydrochloric acid (7.2 mL) and water (1.1 mL) were added. After stirring for a while, sodium nitrite (115.4 mg, 1.68 mmol) was added slowly in 20 min. The result solution was stirred for further 1 hour at 0 ^{o}C. Then the solution was treated with potassium carbonate to pH ≈ 9, and then it was extracted with dichloromethane (3 × 30 mL). After evaporation, the residue was purified by column chromatograph on silica gel eluting with acetonitrile, ethyl acetate and triethylamine (3:1:0.1, v/v/v), to afford product as green solid, 214.5 mg, yield 73.8%. ^{1}H NMR (400 MHz, DMSO-d_6) δ 8.61 (d, J = 2.5 Hz, 1H, Ar-*H*), 8.58 (dd, J = 4.7, 1.1 Hz, 1H, Ar-*H*), 7.87 – 7.84 (m, 1H, Ar-*H*), 7.57 – 7.54 (m, 1H, Ar-*H*), 6.50 (d, J = 2.2 Hz, 1H, Ar-*H*), 6.39 (d, J = 9.4 Hz, 1H, Ar-*H*), 6.06 (dd, J = 9.4, 2.3 Hz, 1H, Ar-*H*), 4.10 (s, 3H, -CH_3), 3.51 (s, 3H, -CH_3). ^{13}C NMR (75 MHz, DMSO-d_6) δ 163.7, 156.5, 155.5, 147.6, 147.4, 141.6, 134.1, 124.2, 110.9, 105.31, 94.7, 55.6, 40.4. HRMS (ESI^{+}): m/z = 244.1081 (calcd for $[M + H^{+}]^{+}$, 244.1086).

2.3.2. *Synthesis of 3-(diethylamino)-7-(pyridin-3-ylamino)phenoxazin-5-ium chloride (**7a**).*

A solution of 3-(diethylamino)phenol (0.99 g, 6.0 mmol) in 90% *i*-PrOH (120.0 mL) was stirred in a distillation apparatus at 70 ^{o}C under a nitrogen atmosphere, then another mixture of **6a** (1.38 g, 6.0 mmol) and hydrochloric acid (6.0 mmol) in *i*-PrOH (120.0 mL) was added within 45 min. The reaction was heated to reflux; when almost 120.0 mL solvent was distilled out, another 90% *i*-PrOH (120.0 mL) was added to the

reaction mixture, this procedure was repeated three times during 3–4 h. The solvent was removed by evaporation. The residue was purified by column chromatograph on silica gel eluting with dichloromethane and methanol (15:1, v/v) to afford product as dark red solid, 0.57 g, yield 25.0%, mp 193.2 – 195.2 ^{o}C. ^{1}H NMR (400 MHz, DMSO-d_6) δ 8.31 (br, 1H, Ar-*H*), 8.15 (br, 1H, Ar-*H*), 7.39 – 7.19 (m, 4H, 4×Ar-*H*), 6.93 (br, 1H, Ar-*H*), 6.74 (br, 1H, Ar-*H*), 6.48 (br, 1H, Ar-*H*), 6.15 (br, 1H, Ar-*H*), 3.46 (br, 4H, 2×-CH_2), 1.13 (br, 6H, 2×-CH_3). ^{13}C NMR (101 MHz, TFA-*d*) δ 161.4, 153.1, 151.6, 150.5, 143.1, 142.9, 139.2, 137.7, 136.6, 134.7, 134.4, 133.2, 130.6, 125.1, 103.8, 100.3, 50.8, 14.1, 13.2. HRMS (ESI$^+$): m/z = 345.1710 (calcd for [M – Cl$^-$]$^+$, 345.1715).

2.3.3. *Synthesis of 3-(diethylamino)-7-(methyl(pyridin-3-yl)amino)phenoxazin-5-ium chloride (**7b**).*

Probe **7b** was synthesized by 3-(diethylamino)phenol (0.99 g, 6.0 mmol) and **6b** (1.46 g, 6.0 mmol) using a similar procedure to probe **7a**. Dark red solid, 0.68 g, yield 28.5% mp 187.5 – 189.5 ^{o}C. ^{1}H NMR (400 MHz, CD_3OD) δ 8.68 (br, 2H, 2×Ar-*H*), 7.98 (br, 1H, Ar-*H*), 7.82 (br, 2H, 2×Ar-*H*), 7.69 (br, 1H, Ar-*H*), 7.59 (br, 1H, Ar-*H*), 7.10 (br, 1H, Ar-*H*), 6.97 (br, 1H, Ar-*H*), 3.88 (br, 4H, 2×-CH_2), 3.67 (br, 4H, 2×-CH_2), 1.40 (br, 6H, 2×-CH_3). ^{13}C NMR (151 MHz, DMSO-d_6) δ 157.6, 156.5, 149.9, 149.1, 148.3, 148.2, 141.7, 137.7, 135.2, 135.0, 133.5, 132.8, 125.4, 120.3, 117.2, 98.2, 96.9, 41.8, 13.5, 12.6. HRMS (ESI$^+$): m/z = 359.1867 (calcd for [M – Cl$^-$]$^+$, 359.1872).

2.4. Optical test of the solutions.

Stock solutions (100 μM) of probes were prepared in a volumetric flask (100 mL) with dimethyl sulfoxide (DMSO). Each test solution was prepared in a volumetric

flask (10 mL) with 1 mL stock solution of probes, diluted with Na_2HPO_4-citric acid buffers (8.0–9.2) which were prepared with 0.2 M Na_2HPO_4 and 0.1 M citric acid and sodium carbonate-sodium bicarbonate buffers (9.4–11.2), which were prepared with 0.1 M Na_2CO_3 and 0.1 M $NaHCO_3$, to give a total volume of 10 mL with different pH values and theoretical pH values of the buffers were used for the buffer solution containing 10% (v/v) DMSO. The resulting solution was shaken for 1 min to form homogeneous solution before the absorption and emission spectra were recorded. All measures were carried out at room temperature, and the excitation and emission slit widths were both 5 nm. Stock solutions of various ions were prepared in volumetric flasks (10 mL) with concentrations of KCl (100 mM), NaCl (100 mM), $CaCl_2$ (0.5 mM), $MgSO_4$ (0.5 mM), $CuSO_4$ (0.3 mM), $MnCl_2$ (0.3 mM), $HgCl_2$ (0.3 mM), $CoCl_2$ (0.3 mM), $NiCl_2$ (0.3 mM), $CdCl_2$ (0.3 mM) in redistilled water; stock solutions of all kinds of amino acids were prepared in volumetric flasks (10 mL) with 0.1 mM solutions of Cys, Gly, Pro, Trp, Glu, Lys, His, Arg and Phe in doubly distilled water. The calculation of the pK_a values for the free dyes was performed using a nonlinear fitting method according to the reported method.[29]

2.5. *Determination of quantum yield.*

All the relative fluorescence quantum yields were determined and calculated with the following equation: $\Phi_x/\Phi_{st} = [A_{st}/A_x][n_x^2/n_{st}^2][D_x/D_{st}]$. Where st: standard; x: sample; Φ: quantum yield; A: absorbance at the excitation wavelength; D: area under the fluorescence spectra on an energy scale; n: the refractive index of the solution calculated from reported data (DMSO/water (v/v = 1/9).[30] The Oxazine **1** dye (Φ =

0.14 in ethanol) was used as standard.[31]

2.6. *Photofading of dyes.*

Probe **7a** was selected to be used for representative photofading of dyes due to all probes were based on the same fluorophore. Test solution (10 μM) was prepared in a volumetric flask (10 mL) with 1 mL stock solution of probe **7a** and sample Oxazine 1, diluted with buffers, to give a total volume of 10 mL with different pH values (pH = 2.0, 7.0, 11.0) were used for the buffer solution containing 10% (v/v) DMSO and dissolved in acetonitrile with a concentration of 10 μM respectively. Solutions of the samples were irradiated with a 500 W Philips iodine–tungsten lamp at room temperature. The distance between the samples and the lamp was 25 cm. An 8 cm thick cold trap (60 $g.L^{-1}$ $NaNO_2$) was set up between the 20 mL transparent glass bottle and the lamp to eliminate the heat and absorb short wavelength light. The photostability was in the terms of remaining absorption (%) calculated from the change of absorption intensity at the absorption maximum before and after irradiation.

2.7. *Cell culture and imaging.*

V79 cells and HeLa cells were cultured with 10% calf serum, penicillin (100 $U{\cdot}mL^{-1}$), streptomycin (100 $\mu g{\cdot}mL^{-1}$) and L-glutamine (2.5×10^{-4} M) at 37 °C in a 5:95 CO^2-air incubator and the cells with 2×10^5 density were incubated on glass-bottomed coverslip of 35 mm for two days before imaging. To the cells in coverslip with 1.0 mL PBS, LysoTracker Green DND-26 (final concentration 50 nM) and probes **7a–b** (final concentration 10 μM) were added, and cells were further

incubated for 15 min. After the stained cells were washed twice with phosphate-buffered saline (PBS), fluorescence confocal images of the stained cells were obtained. The confocal fluorescence imaging was performed by microscope with 20× objective lens. Green channel was excited at 488 nm and emission was collected at 505–550 nm; red channel was excited at 581 nm, and emission was collected in 590–790 nm. The images and fluorescence intensity were handled with LAS-AF lite software.

2.8. *CCK-8 assay for the cell cytotoxicity.*

Dispense 100 µL of HeLa or V79 cells suspension (5000 cells/well) in a 96-well plate. Pre-incubate the plate for 24 hours in a humidified incubator (at 37°C, 5% CO_2). Then 10 µL various concentrations of (2 µM, 5 µM, 10 µM, 12 µM, 15 µM, and 20 µM) of probes **7a** and **7b** were added to the plate respectively and Incubated for 6 hours in the incubator. The 10 µL of CCK-8 solution was added to each well of the plate, and then the plate was incubated for 1 hour in the incubator. The cell viability was calculated as a percentage using the following formula: survival rate (%) = $(A_{sample}-A_b)$ / (A_c-A_b). (A_c: Negative control (including media and cells, no test substance), A_b: blank (including test substance and media, no cells)).

3. Result and discussion

3.1. Preparation of phenoxazinium with nitrophenyl groups (3a–c)

The designed synthetic route of probes **3a-c** is shown in scheme 1. Phenoxazinium skeleton was selected to give the comparative evaluation with benzo[a]phenoxazine, *o*-nitrophenyl (**3a**), *m*-nitrophenyl (**3b**) and *p*-nitrophenyl (**3c**)

groups were used to explore the influence of different electron withdrawing groups. Briefly, 3-methoxyl-*N*-nitrophenylaniline (**1a–c**) was treated with sodium nitrite under hydrochloric acid conditions to give 3-methoxy-*N*-nitrophenyl-4-nitrosoaniline (**2a–c**), which reacted with 3-(diethylamino)-phenol in the mixture of hydrochloric acid and 90% isopropyl alcohol under nitrogen atmosphere to give the target molecules (**3a–c**).[32] The deprotonated and protonated equilibriums of **3a–c** will be occurred between phenoxazinium and the corresponding phenoxazine. The PET will not be allowed from the positive charged phenoxazinium to the electron withdrawing nitrophenyl group; while the electron could transfer from the deprotonated electroneutral phenoxazine to nitrophenyl group, and PET process is allowed and their emission response could be detected.[33]

Scheme 1.

3.2. Absorption and emission properties of probes 3a–c

The absorption spectra of **3a–c** (10 μM) in various disodium hydrogen phosphate-citric acid (8.0–9.2) and sodium carbonate-sodium bicarbonate buffers (9.4–10.8) containing 10% DMSO were tested. The absorption maximum of **3a** at 560 nm (Fig. 1(a), pH = 10.8, ε = 1.79 × 10^4 M^{-1} cm^{-1}) red-shifted to 630 nm (pH = 8.0, ε = 3.27 × 10^4 M^{-1} cm^{-1}) with the increasing acidity, accompanied by the color of the solution change from light blue to sky blue. Probe **3b** produced an absorption maximum at 583 nm (Fig. S1(a), pH = 10.8, ε = 1.76 × 10^4 M^{-1} cm^{-1}), and red-shifted to 638 nm (pH = 8.0, ε = 4.82 × 10^4 M^{-1} cm^{-1}). The absorption of probe **3c** exhibited a relative small hypochromatic shift from 602 nm (Fig. S1(c), pH = 10.8, ε = 2.09 × 10^4

M^{-1} cm^{-1}) to 640 nm (pH = 8.0, ε = 5.83 × 10^4 M^{-1} cm^{-1}). Regarding to the absorption and excitation spectra (Fig. 1(c), and Fig. S2), the excitation wavelengths were selected at 633 nm, 635 nm, and 638 nm for probes **3a–c** in order to obtain appropriate emission spectra in the next stage.

Fig. 1.

Fluorescent pH titration experiments indicated that probes **3a–c** were nearly OFF-ON type responses from pH = 10.8 to pH = 8.0. The weak emission maximum of probe **3a** in its deprotonated form was located at 646 nm (Fig. 1(b)), and the emission of its protonated form was determined to be 676 nm with a full range of emission at 650–850 nm; the relative fluorescent intensity increased 15.7 times, the calculated pK_a value was 8.7. Probes **3b–c** had the similar emission properties with **3a**, the relative fluorescent intensity of **3b** increased 12.2 times from 648 nm at pH = 10.8 to 685 nm at pH = 8.0 (Fig. S1(b)); the deprotonated form of **3c** gave emission at 652 nm, and it red-shifted to 693 nm, the fluorescent intensity increased 16.3 times (Fig. S1(d)). The pK_a of **3c** was close to the value of **3a**, while **3b** had a relative higher pK_a at 9.2. Further optical tests in alternating pH 8.0 and 10.8 indicated that the absorptions and emissions of probes **3a–c** were reversible (Fig. S3).

Table 1.

The nitrogroups in **3a** and **3c** have electron withdrawing conjugative and inductive effects towards the attached amino groups, while only inductive effect between nitrogroup and amino group exists in **3b**, the optical properties of **3a–c** with different nitrophenyl groups disclosed that the strong electron withdrawing

N-substituted groups enhance the deprotonated processes of phenoxazinium. Compared with the reported benzo[a]phenoxazine, the phenoxazinium derivatives with *N*-nitrophenyl groups exhibit the higher pK_as, which indicates the pH response ranges are greatly influenced by the benzo[a]phenoxazine heterocycles, and the smaller conjugated system of phenoxazinium gives less chance of the deprotonation. The photochemical properties of the three probes were summarized in Table 1. Although the phenoxazinium with nitrophenyl groups give nearly OFF-ON emission towards pH, the weak fluorescent intensities and the high pK_as are rather unfavorable to lysosomal probes for cancer cells. Therefore, the optimization measure is still required to improve their photochemical properties.

3.3. Preparation of phenoxazinium with pyridinyl group (7a–b)

Phenoxazinium with pyridinyl group (**7a**) was designed to improve the optical properties, because the introduction of pyridinyl group will renders reduction of pK_a value and at the same time as electron-withdraw group similar with compound **3a–c**. The preparation of probe **7a** is shown in Scheme 2. Compound **5a** was synthesized by one-step procedure from 1-iodo-3-methoxybenzene and 3-aminopyridine,[34] and then compound **6a** was prepared by nitrosification of compound **5a**. The final product (probe **7a**) was synthesized by the condensation of compound **6a** and *m*-(diethylamino)-phenol in acidic isopropanol solution. Probe **7b** was obtained by the similar way to verify the protonated and deprotonated mechanism, a methylated step from **5a** to **5b** was added to obtain the desired compound. The structures of all compounds were confirmed by ^{1}HNMR, ^{13}CNMR and high resolution mass (ESI^{+})

spectroscopies.

Scheme 2.

3.4. Absorption and emission properties of probes 7a–b

Absorption and fluorescence pH titration experiments of **7a–b** (10 μM) were performed in various hydrochloric acid-citric acid buffer (pH = 1.2), disodium hydrogen phosphate-citric acid buffer (pH = 1.6–9.2), and disodium hydrogen phosphate-sodium carbonate buffer (pH = 9.4–11.2) containing 10% DMSO. From Fig. 2(a), when pH reduced from 11.2 to 1.2, the absorption maximum of probe **7a** at 636 nm decreased, and a new absorption maximum at 580 nm gradually increased, accompanied by light blue changed to dark blue of test solution (10 mL) which contain 1 mL stock solution. The excitation wavelength was selected at 585 nm according to excitation spectra (Fig. 2(c)), probe **7a** showed two-stage changes at pH 1.2–6.4 and pH 6.4–11.2 (Fig. 2(b), Fig. S4). When pH decreased from 6.4 to 1.2, emission spectra of dye **7a** towards pH showed a nearly OFF-ON fluorescence response, the result could attributed to protonation of pyridine (from **7a** to **7a**+H^+, Scheme 2, and the PET process from the pyridine group to the phenoxazinium ring is prohibited, and nearly OFF–ON type response of probe **7a** towards pH (Fig. 2b) could be detected. The deprotonation process of **7a** was happened in basic condition, emission peak of probe **7a** slightly reduced from pH 6.4 to pH 11.2 (Fig. S4(a)). The calculated pK_a values of probe **7a** towards pH were 3.71 and 9.68 at pH 1.2–6.4 and pH 6.4–11.2 respectively (Fig. 3(d), Fig. S4(c)). To further verify the deprotonation of phenoxazinium in pH range of 6.4–11.2, probe **7b** was prepared for the evaluation of

pH related emission response.

From Fig. 3(a), the absorption maximum of probe **7b** at 643 nm was gradually blue-sifted to 592 nm when pH reduced from 6.4 to 1.2. The excitation wavelength was selected at 595 nm according to excitation spectra (Fig. 3(c)), only one step fluorescent response was found in emission spectra. The calculated pK_a value of probe **7b** was 2.75 (Fig. 3d). A summary of optical changes of probes **7a** and **7b** towards pH were listed in Table 2. Compared the properties of probes **3a–c** in Table 1, fluorescence quantum yields of probe **7a** and **7b** in their protonated forms have been significantly improved. The results indicated that pyridinyl groups have advantage over anilino groups in probe design.

Fig. 2.

Fig. 3.

Table 2.

Probes **7a** and **7b** possess the lower pK_as and will be suitable for living cell detection. Therefore, the reversibility of probes **7a** and **7b** was evaluated. When solution of probe **7a** was changed to acidity or basic conditions and that of probe **7b** was alternated to acidity or neutral conditions for five cycles, the emission spectra have no significant changes (Fig. S5). It can be deduced that probes **7a** and **7b** have good reversibility.

The selectivity of probes **7a–b** for other potential interferents under biological conditions was also investigated at different pH conditions. As shown in Fig. S6 and Fig. S7, no significant changes were observed in fluorescence intensity of probes **7a**

and **7b** (10 μM) in the presence of common cations such as K^+, Na^+, Ca^{2+} and Mg^{2+}, as well as heavy or transition-metal ions, such as Cd^{2+}, Cu^{2+}, Co^{2+}, Hg^{2+}, Mn^{2+}, and Ni^{2+}. Moreover, bioactive amino acids, such as Lys, Phe, Gly, Glu, Arg, Cys, Pro, Try, and His. The results illustrated that probes **7a** and **7b** with good selectivity response to H^+ in the presence of common cations, metal ions and amino acids.

The photostability of probe **7a** in acetonitrile and buffers with different pH values (pH = 2, 7 and 11) containing 10% DMSO was investigated respectively for representative due to all dyes were based on the same fluorophore, and Oxazine 1 also studied as standard samples in acetonitrile and buffers for comparison. As shown in Fig. S8, the remaining absorptions of probe **7a** and Oxazine 1 both were more than 97% in acetonitrile after 5 hours of irradiation while the remaining absorptions of probe **7a** and Oxazine 1 were only 41% in buffers of pH = 11. The results indicated that probe **7a** is more stable in acetonitrile than strong alkaline buffers, and the phenoxazinium fluorophore has excellent light stability in acetonitrile and weak base conditions.

3.5. CCK-8 assay for the cell cytotoxicity

The CCK-8 assay of probes **7a–b** in V79 and HeLa cells were first studied. As shown in Fig. 4, after 6 hours of cellular internalization of the probe at a concentration of 12 μM, more than 92% cells were viable with **7a–b**. With the concentration increased to 20 μM, the cell viability remained more than 72%. The results indicate the low cytotoxicity of **7a–b**, which is more suitable for fluorescence imaging of living cells.

Fig. 4.

3.6. Fluorescence imaging of living cells with probes 7a−b

Fluorescence confocal images of V79 cells and HeLa cells with probe **7a** were performed firstly. The V79 cells (Fig. 5(a–d)) and HeLa cells (Fig. 5(e–h)) were incubated with probe **7a** (10 μM) and LysoTracker Green DND-26 (50 nM) for 15 min respectively. As shown in Fig. 4, green channel images (Fig. 5(b, f)) from LysoTracker Green DND-26 gave the location of lysosomes, and red channel images (Fig. 5(c, g)) from probe **7a** were also obtained. From the overlay images of green channels and red channels (Fig. 5(d, h)), it indicated that probe **7a** was a lysosomal targetable probe. The fluorescence intensities of the regions of interest (ROIs, Fig. 5(i) from Fig. 5(b) and Fig. 5(c) across V79 cells, Fig. 5(j) from Fig. 5(f) and Fig. 5(g) across HeLa cells) also confirmed that the red channel of probe **7a** was well overlapped with the green channel of LysoTracker Green. The results illustrate that probe **7a** was a good lysosome-targetable pH probe. Probe **7b** was also used for the staining of V79 and HeLa cells (Fig. S9), however, only slightly background emission was detected, and probe **7b** was thus not suit for a biomarker, which assumed that the smaller pK_a value of probe **7b** was not suitable been applied for lysosome of V79 and Hela cells.

Fig. 5.

4. Conclusion

Phenoxazinium with nitrophenyl groups (**3a–c**) were prepared, they have pH achievable NIR emission responses by equilibrium between phenoxazinium and phenoxazine; these dyes have higher pK_as in the alkaline environment within pH 8.0–

10.8. Phenoxazinium with pyridinyl group (**7a–b**) were prepared to improve the emission properties, the equilibrium between phenoxazine and phenoxazinium gave responsible emission at pH 6.4–12.0; the protonated process of pyridinyl group gave responsible emission at pH 1.2–6.4, and exhibited the relative strong emission. All the probes are reversible to pHs, and probe **7a** and **7b** possess good selectivity, excellent photostability and low cell cytotoxicity. Probe **7a** is a lysosome biomarker for V79 and HeLa cells. Of course, the pH working interval of fluorescence pH probes can be expanded by molecular design so as to be used for biological detection.

Acknowledgements

This work was financially supported by Natural Science Fund of Jiangsu Province in China (BK20151262), the National Natural Science Foundation of China (51273136), a project funded by the Priority Academic Program Development of Jiangsu Higher Education Institutions (PAPD) and the project of scientific and technologic infrastructure of Suzhou (SZS201708).

Appendix. Supplementary data

Supplementary data associated with this article can be found, in the online version.

References

[1] Rouse J, Jackson SP. Interfaces Between the Detection, Signaling, and Repair of DNA Damage. Science 2002;297(5581):547-51.

[2] Maji R, Mahapatra AK, Maiti K, Mondal S, Ali SS, Sahoo P, et al. A highly sensitive fluorescent probe for detection of hydrazine in gas and solution phases based on the

Gabriel mechanism and its bioimaging. RSC Adv 2016;6(75):70855-62.

[3] Zhang X, Li D, Qin J, Xu Y, Ma K. Synthesis of 4-thio-5-(2′′-thienyl)uridine and cytotoxicity activity against colon cancer cells in vitro. RSC Adv 2016;6(74):70099-105.

[4] Ter Weele EJ, Terwisscha van Scheltinga AG, Linssen MD, Nagengast WB, Lindner I, Jorritsma-Smit A, et al. Development, preclinical safety, formulation, and stability of clinical grade bevacizumab-800CW, a new near infrared fluorescent imaging agent for first in human use. Eur J Pharm Biopharm 2016;104:226-34.

[5] Karanikola SN, Krucken J, Ramunke S, de Waal T, Hoglund J, Charlier J, et al. Development of a multiplex fluorescence immunological assay for the simultaneous detection of antibodies against Cooperia oncophora, Dictyocaulus viviparus and Fasciola hepatica in cattle. Parasite Vector 2015;8:335.

[6] Lu YJ, Hu DP, Zhang K, Wong WL, Chow CF. New pyridinium-based fluorescent dyes: A comparison of symmetry and side-group effects on G-Quadruplex DNA binding selectivity and application in live cell imaging. Biosens Bioelectron 2016;81:373-81.

[7] Kovalska V, Chernii S, Losytskyy M, Dovbii Y, Tretyakova I, Czerwieniec R, et al. beta-ketoenole dyes: Synthesis and study as fluorescent sensors for protein amyloid aggregates. Dyes Pigm 2016;132:274-81.

[8] Xiao HB, Zhang YZ, Zhang W, Li SZ, Xu RH. Two novel dyes containing spirobifluorene and triphenylamine: Synthesis, one- and two-photon excited fluorescence and applications as probes for silver ions, water and cell imaging. Sens

Actuators B 2016;233:469-75.

[9] Li BH, Zhang YL, Li FS, Wang W, Liu J, Liu M, et al. A novel sensor for the detection of alkaline phosphatase activity based on the self-assembly of Eu3+-doped oxide nanoparticles and heptamethine cyanine dye. Sens Actuators B 2016;233:479-85.

[10] Chen X, Lin C, Chen Y, Luo F, Wang Y, Chen X. Terminal protection of a small molecule-linked loop DNA probe for turn-on label-free fluorescence detection of proteins. Biosens Bioelectron 2016;83:97-101.

[11] Yue Y, Huo F, Lee S, Yin C, Yoon J. A review: the trend of progress about pH probes in cell application in recent years. Analyst 2016;142(1):30-41.

[12] Dong BL, Song XZ, Kong XQ, Wang C, Zhang N, Lin WY. A tumor-targeting and lysosome-specific two-photon fluorescent probe for imaging pH changes in living cells. J Mater Chem B 2017;5(5):988-95.

[13] Yuan L, Lin W, Zheng K, He L, Huang W. Far-red to near infrared analyte-responsive fluorescent probes based on organic fluorophore platforms for fluorescence imaging. Chem Soc Rev 2013;42(2):622-61.

[14] Chen H, Dong B, Tang Y, Lin W. A Unique "Integration" Strategy for the Rational Design of Optically Tunable Near-Infrared Fluorophores. Acc Chem Res 2017;50(6):1410-22.

[15] Deniz E, Isbasar GC, Bozdemir OA, Yildirim LT, Siemiarczuk A, Akkaya EU. Bidirectional switching of near IR emitting boradiazaindacene fluorophores. Org Lett 2008;10(16):3401-3.

[16] Tang B, Yu F, Li P, Tong L, Duan X, Xie T, et al. A near-infrared neutral pH

fluorescent probe for monitoring minor pH changes: imaging in living HepG2 and HL-7702 cells. J Am Chem Soc 2009;131(8):3016-23.

[17] Dong B, Song X, Wang C, Kong X, Tang Y, Lin W. Dual Site-Controlled and Lysosome-Targeted Intramolecular Charge Transfer-Photoinduced Electron Transfer-Fluorescence Resonance Energy Transfer Fluorescent Probe for Monitoring pH Changes in Living Cells. Anal Chem 2016;88(7):4085-91.

[18] Zhu H, Fan J, Xu Q, Li H, Wang J, Gao P, et al. Imaging of lysosomal pH changes with a fluorescent sensor containing a novel lysosome-locating group. Chem Commun 2012;48(96):11766-8.

[19] Fan L, Fu YJ, Liu QL, Lu DT, Dong C, Shuang SM. Novel far-visible and near-infrared pH probes based on styrylcyanine for imaging intracellular pH in live cells. Chem Commun 2012;48(91):11202-4.

[20] Deng M, Yang CD, Gong DY, Iqbal A, Tang XL, Liu WS, et al. BODIPY-derived piperazidine fluorescent near-neutral pH indicator and its bioimaging. Sens Actuators B 2016;232:492-8.

[21] Zhan YH, Liu W, Sun R, Li XS, Ge JF. Diaminodibenzoxanthenium based near infrared pH probes with lower pK(a). Dyes Pigm 2016;132:223-9.

[22] Saleh SM, Ali R, Elshaarawy RFM. A ratiometric and selective fluorescent chemosensor for Ca(II) ions based on a novel water-soluble ionic Schiff-base. RSC Adv 2016;6(73):68709-18.

[23] Niu WF, Fan L, Nan M, Wong MS, Shuang SM, Dong C. A novel fluorescent probe for sensing and imaging extreme acidity. Sens Actuators B 2016;234:534-40.

[24] Faggi E, Serra-Vinardell J, Pandey MD, Casas J, Fabrias G, Luis SV, et al. Pseudopeptidic fluorescent on-off pH sensor based on pyrene excimer emission: Imaging of acidic cellular organelles. Sens Actuators B 2016;234:633-40.

[25] Mizukawa Y, Ge JF, Bakar Md A, Itoh I, Scheurer C, Wittlin S, et al. Novel synthetic route for antimalarial benzo[a]phenoxazine derivative SSJ-183 and two active metabolites. Bioorg Med Chem 2014;22(14):3749-52.

[26] He DD, Liu W, Sun R, Fan C, Xu YJ, Ge JF. N-Pyridineium-2-yl Darrow Red analogue: unique near-infrared lysosome-biomarker for the detection of cancer cells. Anal Chem 2015;87(3):1499-502.

[27] Liu W, Fan C, Sun R, Xu YJ, Ge JF. Near-infrared emission of dibenzoxanthenium and its application in the design of nitric oxide probes. Org Biomol Chem 2015;13(15):4532-8.

[28] Ge JF, Arai C, Kaiser M, Wittlin S, Brun R, Ihara M. Synthesis and in vitro antiprotozoal activities of water-soluble, inexpensive 3,7-bis(dialkylamino)phenoxazin-5-ium derivatives. J Med Chem 2008;51(12):3654-8.

[29] Povrozin YA, Markova LI, Tatarets AL, Sidorov VI, Terpetschnig EA, Patsenker LD. Near-infrared, dual-ratiometric fluorescent label for measurement of pH. Anal Biochem 2009;390(2):136-40.

[30] Rurack K, Spieles M. Fluorescence quantum yields of a series of red and near-infrared dyes emitting at 600-1000 nm. Anal Chem 2011;83(4):1232-42.

[31] Markarian SA, Terzyan AM. Surface tension and refractive index of dialkylsulfoxide plus water mixtures at several temperatures. J Chem Eng Data

2007;52(5):1704-9.

[32] Ge JF, Arai C, Ihara M. The convenient synthesis of zinc chloride-free 3,7-bis(dialkylamino)phenoxazinium salts. Dyes Pigm 2008;79(1):33-9.

[33] Zhan YH, Li XJ, Sun R, Xu YJ, Ge JF. Distinguishing normal cells from cancer cells via lysosome-targetable pH biomarkers with benzo[a]phenoxazine skeleton. Anal Chim Acta 2016;933:175-81.

[34] Mu B, Li JY, Wu YJ. Carbene adduct of cyclopalladated ferrocenylimine-assisted synthesis of aminopyridine derivatives by the amination of chloropyridines with primary and secondary amines. Appl Organomet Chem 2013;27(9):537-41.

Figure caption:

Scheme 1. Preparation and the protonated and deprotonated processes of probes **3a–c**.

Scheme 2. Preparation and the protonated and deprotonated processes of probes **7a–b**.

Figure 1. pH promoted absorption and emission properties of probes **3a–c** (10 μM) in disodium hydrogen phosphate-citric acid buffers (8.0−9.2) and sodium carbonate-sodium bicarbonate buffers (9.4−10.8) containing 10% DMSO: (a) absorption spectra of dye **3a**, the insert is pH-dependent photograph of the sample; (b) emission spectra of **3a** (λ_{ex} = 633 nm); (c) excitation spectra of probe **3a** (λ_{em} = 688 nm, slit: 5 nm/5 nm) in pH 8.0 and 10.8; (d) normalized fluorescence intensities of probes **3a–c** in different pHs at 676 nm (probe **3a**), 685 nm (probe **3b**), and 693 nm (probe **3c**).

Figure 2. Optical responses of probe **7a** (10 μM) towards various pHs with buffer solution containing 10% DMSO: (a) absorption spectra; (b) emission spectra (λ_{ex} = 585 nm, slit: 3 nm/5 nm,); (c) excitation spectra (λ_{em} = 688 nm, slit: 3 nm/5 nm); (e) fluorescence intensity changes towards pHs at maximum emission peak. Details of probe **7a** in pH 6.4–12.0 were shown in Fig. S4.

Figure 3. Optical responses of probe **7b** (10 μM) towards various pHs with buffer solution containing 10% DMSO: (a) absorption spectra; (b) emission spectra (λ_{ex} = 595 nm, slit: 3 nm/5 nm); (c) excitation spectra (λ_{em} = 688 nm, slit: 5 nm/5 nm); (e) fluorescence intensity changes towards pHs at maximum emission peak.

Figure 4. Percentages of HeLa cell viabilities remaining after cell treatment with probes **7a–b** (untreated cells were considered to have 100% survival). (a) Probe **7a**. (b) Probe **7b**. Cell viabilities were assayed by the CCK-8 method.

Figure 5. Fluorescence confocal images of V79 and HeLa cells with LysoTracker Green DND-26 (50 nM) and probe **7a** (10 μM). (a−d) V79 cells; (e−h) HeLa cells; (a, e) bright-field images; (b, f) green channel emission, collected in 505–550 nm upon excitation at 488 nm; (c, g) red channel emission, collected in 590–790 nm upon excitation at 581 nm; (d) overlay of (b) and (c); (h) overlay of (f) and (g); (i) fluorescence intensities of the ROI across V79 cells; (j) fluorescence intensities of the ROI across HeLa cells.

Table 1. Photochemical properties of probes **3a–c**.

Table 2. Photochemical properties of probes **7a–b**.

Table 1. Photochemical properties of probes **3a–c**.

Entry	$\lambda_{Abs,\ max}$ /nm	$\lambda_{Em,\ max}$ /nm	Stokes shift/nm	ε /M^{-1}·cm^{-1}	Φ [a] /%	pK_a [d]
3a - H^+	560	646	86	1.79×10^4	0.08 [b]	8.7
3a	630	676	46	3.27×10^4	0.12 [c]	
3b - H^+	583	648	65	1.76×10^4	0.07 [b]	9.2
3b	638	685	47	4.82×10^4	0.17 [c]	
3c - H^+	602	652	50	2.09×10^4	0.07 [b]	8.9
3c	640	693	53	5.83×10^4	0.10 [c]	

[a] Oxazine **1** (Φ = 0.14, ethanol) was used as the reference for fluorescence quantum yields. [b] The deprotonated forms were tested in buffer solution (pH = 10.8) containing 10% DMSO. [c] Tested in buffer solution (pH = 8.0) containing 10% DMSO. [d] Calculated by emission spectra.

Table 1. Photochemical properties of probes **7a–b**.

Entry	$\lambda_{Abs,\ max}$ /nm	$\lambda_{Em,\ max}$ /nm	Stokes shift/nm	ε /M⁻¹·cm⁻¹	Φ [a] /%	pK_a [e]
7a - H^+	636	689	53	8.48×10^4	0.07 [b]	3.71, 9.68
7a + H^+	580	664	84	6.22×10^4	0.83 [c]	
7b	643	675	32	4.50×10^4	0.17 [d]	2.75
7b + H^+	592	667	75	2.67×10^4	0.43 [c]	

[a] Oxazine **1** (Φ = 0.14, ethanol) was used as the reference for fluorescence quantum yields. [b] The deprotonated forms were tested in buffer solution (pH = 11.2) containing 10% DMSO. [c] The protonated forms were tested in buffer solution (pH = 1.2) containing 10% DMSO. [d] Test in buffer solution (pH = 6.4) containing 10% DMSO. [e] Calculated by emission spectra.

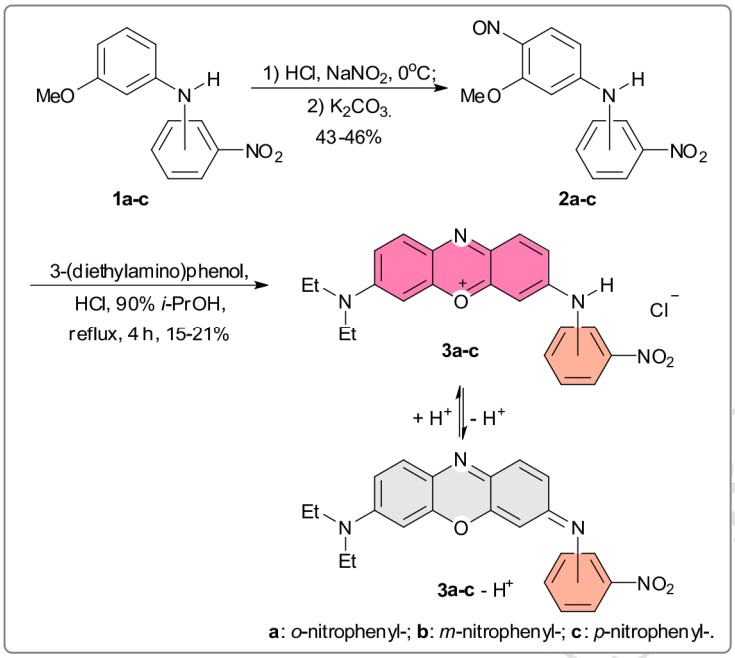

Scheme 1. Preparation and the protonated and deprotonated processes of probes **3a–c**.

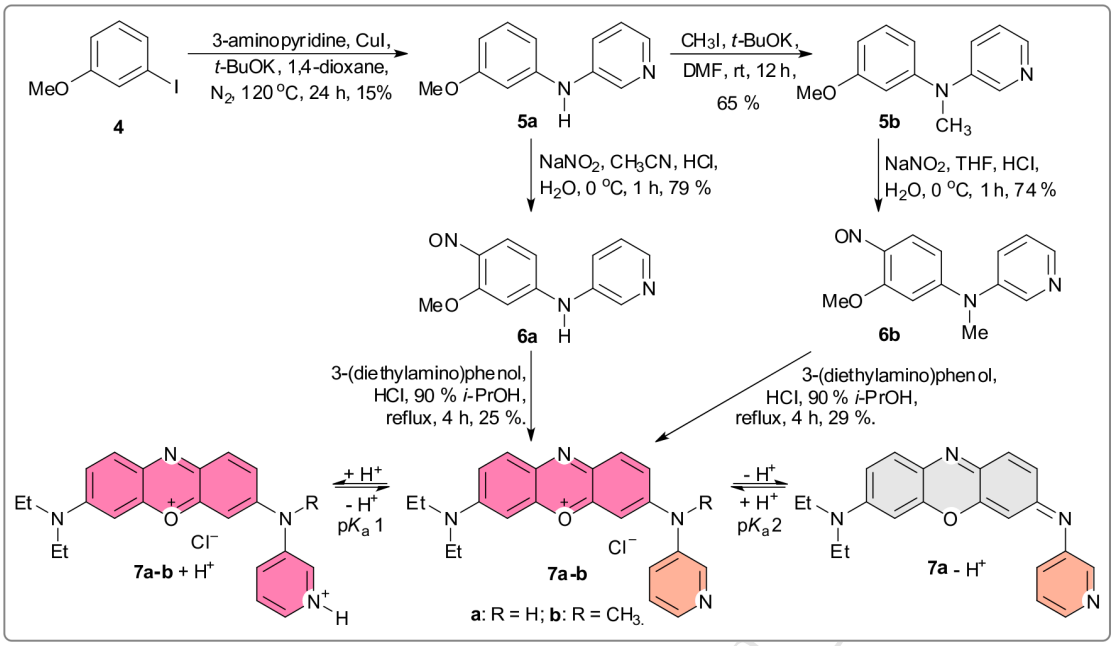

Scheme 2. Preparation and the protonated and deprotonated processes of probes **7a–b**.

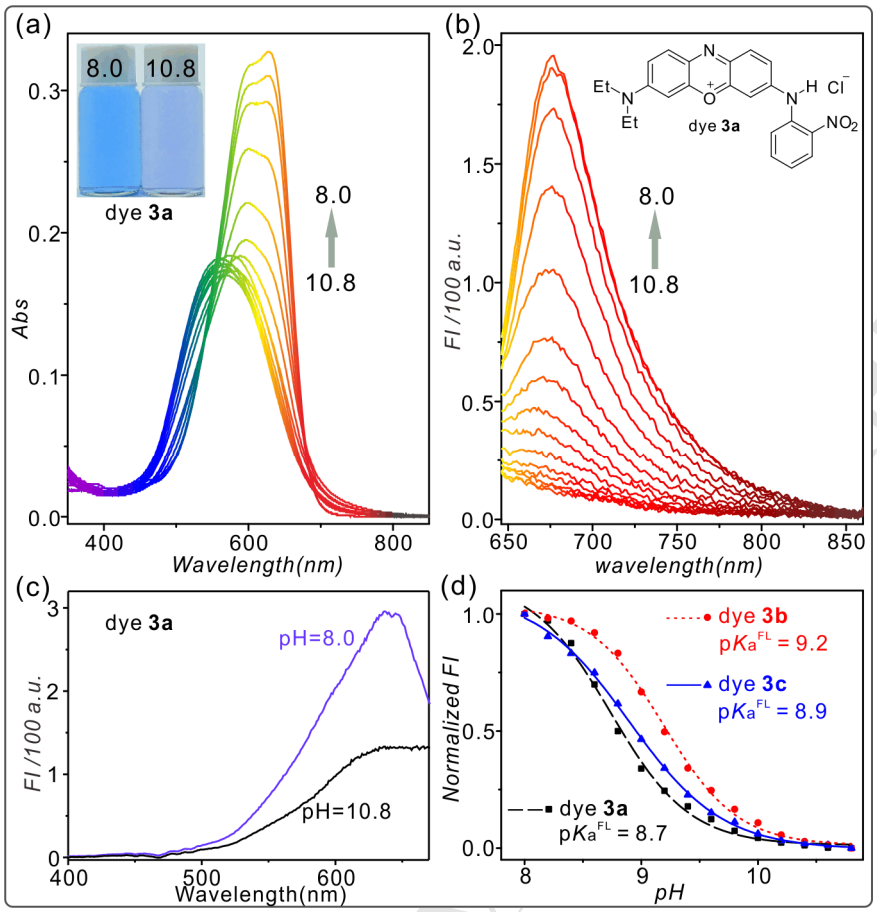

Fig. 1. pH promoted absorption and emission properties of probes **3a–c** (10 μM) in disodium hydrogen phosphate-citric acid buffers (8.0–9.2) and sodium carbonate-sodium bicarbonate buffers (9.4−10.8) containing 10% DMSO: (a) absorption spectra of dye **3a**, the insert is pH-dependent photograph of the sample; (b) emission spectra of **3a** (λ_{ex} = 633 nm); (c) excitation spectra of probe **3a** (λ_{em} = 688 nm, slit: 5 nm/5 nm) in pH 8.0 and 10.8; (d) normalized fluorescence intensities of probes **3a–c** in different pHs at 676 nm (probe **3a**), 685 nm (probe **3b**), and 693 nm (probe **3c**).

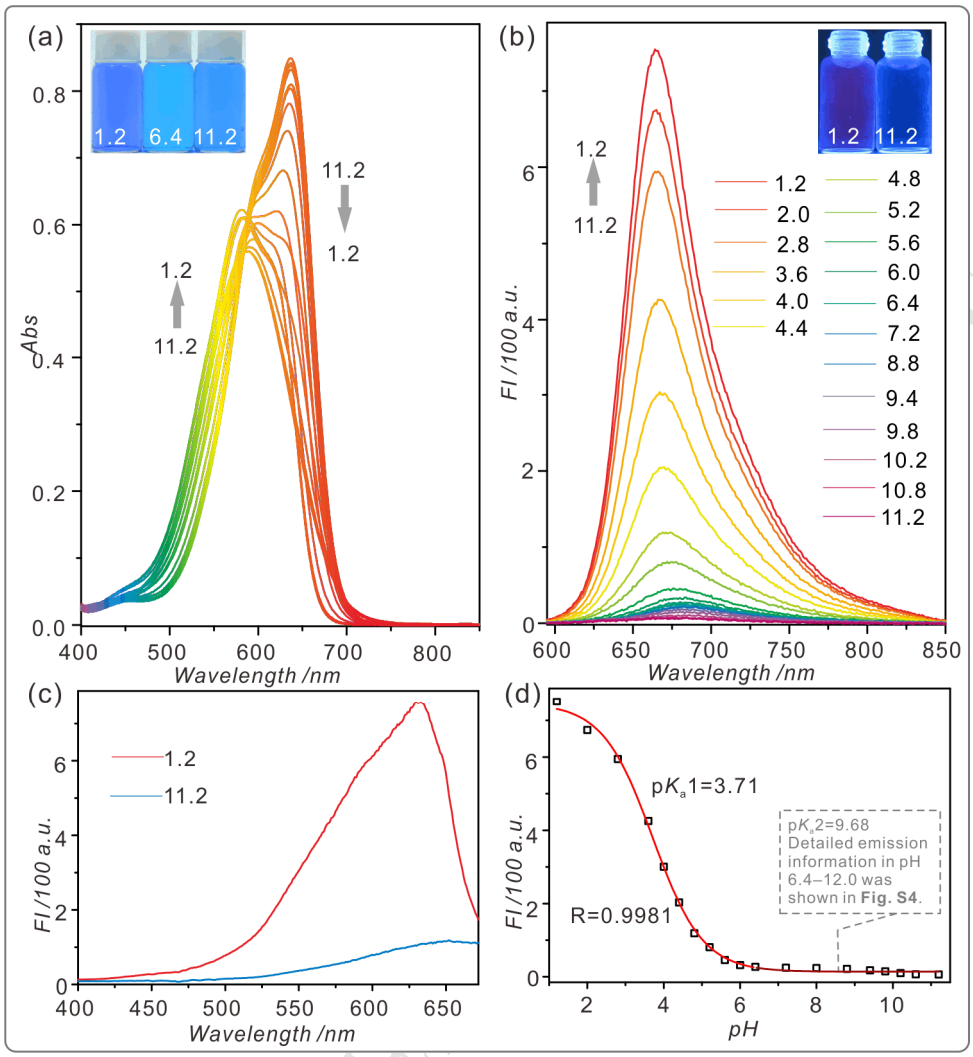

Fig. 2. Optical responses of probe **7a** (10 μM) towards various pHs with buffer solution containing 10% DMSO: (a) absorption spectra; (b) emission spectra (λ_{ex} = 585 nm, slit: 3 nm/5 nm,); (c) excitation spectra (λ_{em} = 688 nm, slit: 3 nm/5 nm); (e) fluorescence intensity changes towards pHs at maximum emission peak. Details of probe **7a** in pH 6.4–12.0 were shown in Fig. S4.

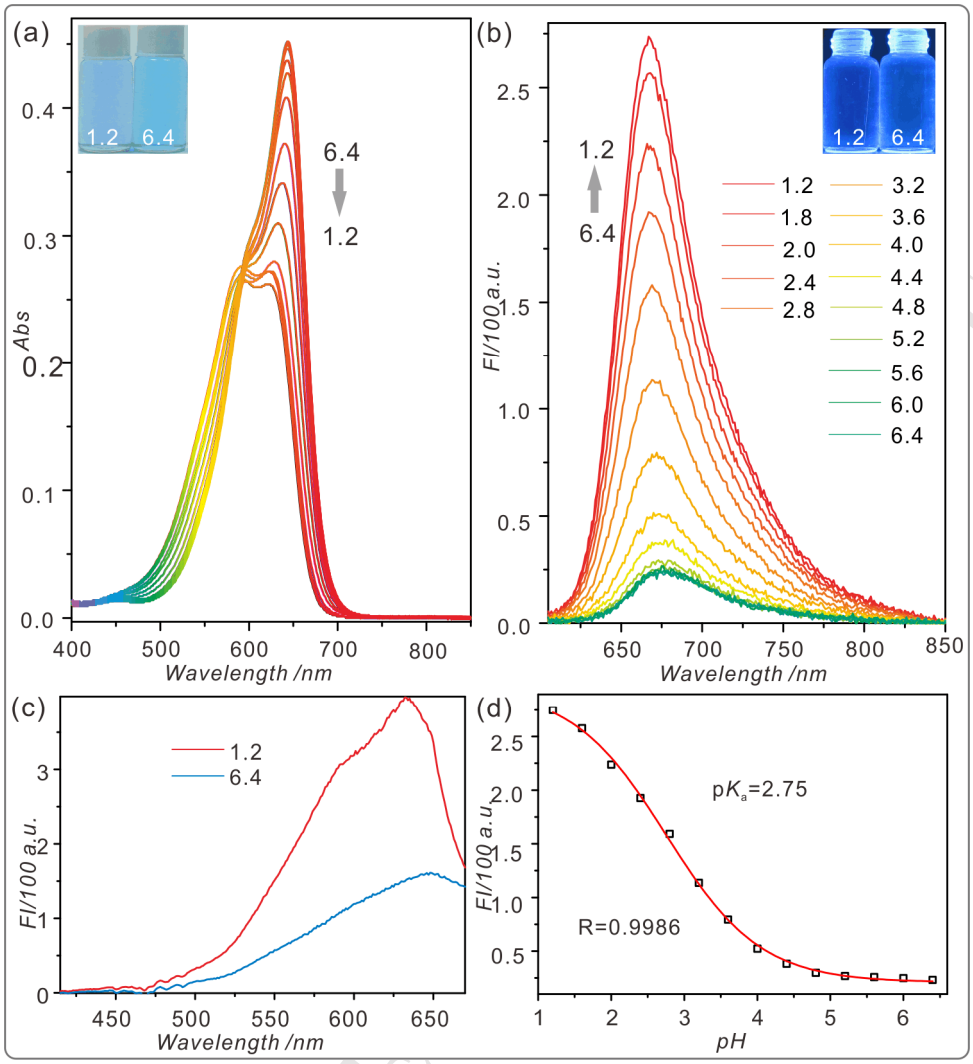

Fig. 3. Optical responses of probe **7b** (10 μM) towards various pHs with buffer solution containing 10% DMSO: (a) absorption spectra; (b) emission spectra (λ_{ex} = 595 nm, slit: 3 nm/5 nm); (c) excitation spectra (λ_{em} = 688 nm, slit: 5 nm/5 nm); (e) fluorescence intensity changes towards pHs at maximum emission peak.

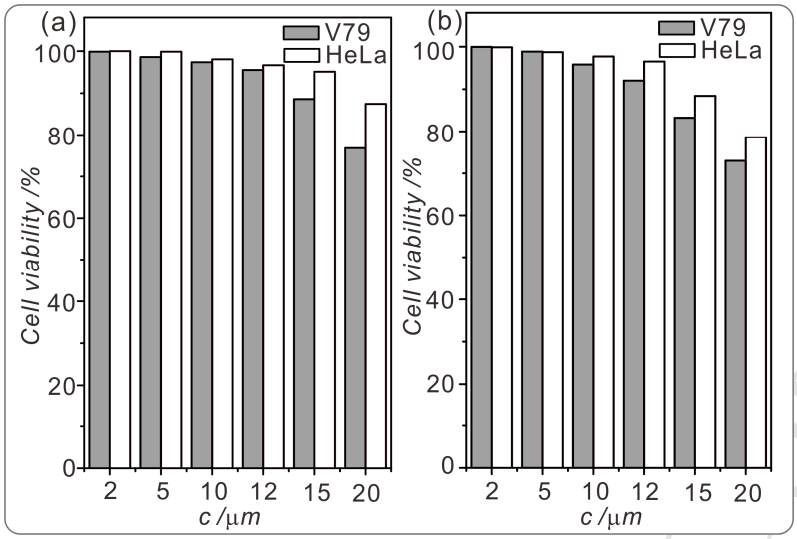

Fig. 4. Percentages of HeLa cell viabilities remaining after cell treatment with probes **7a–b** (untreated cells were considered to have 100% survival). (a) Probe **7a**. (b) Probe **7b**. Cell viabilities were assayed by the CCK-8 method.

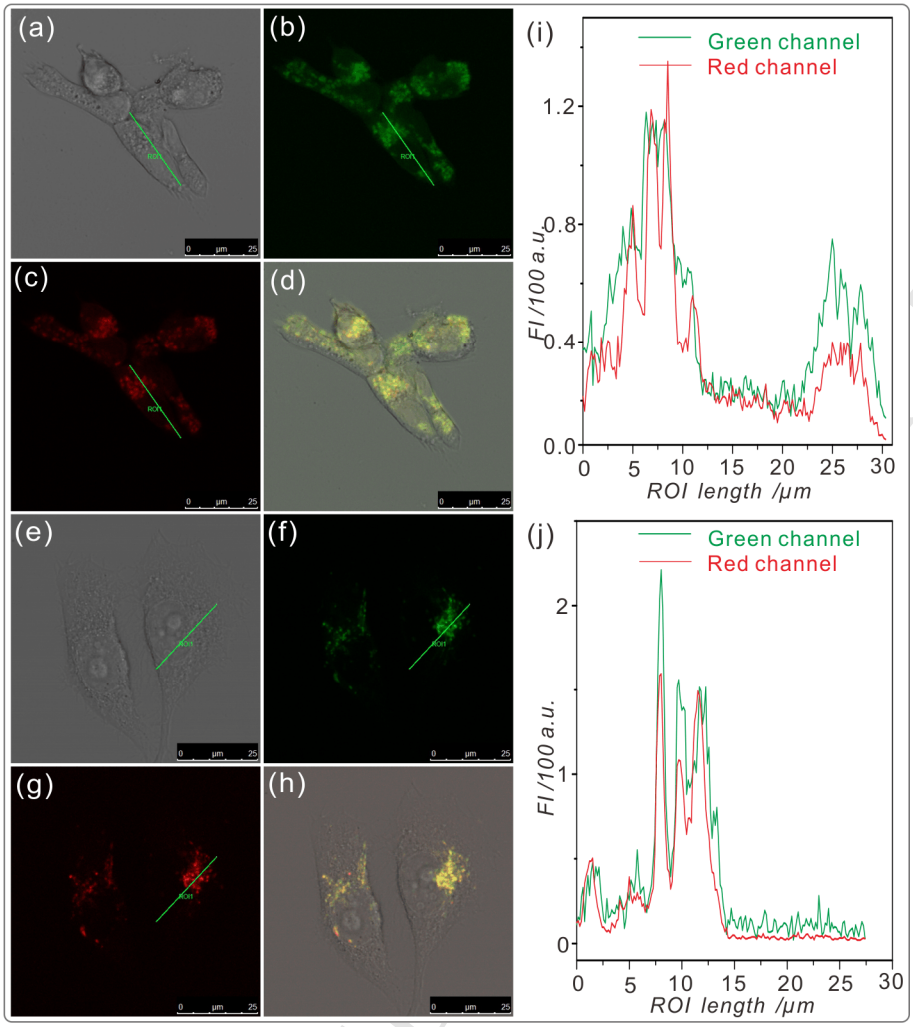

Fig. 5. Fluorescence confocal images of V79 and HeLa cells with LysoTracker Green DND-26 (50 nM) and probe **7a** (10 μM). (a–d) V79 cells; (e–h) HeLa cells; (a, e) bright-field images; (b, f) green channel emission, collected in 505–550 nm upon excitation at 488 nm; (c, g) red channel emission, collected in 590–790 nm upon excitation at 581 nm; (d) overlay of (b) and (c); (h) overlay of (f) and (g); (i) fluorescence intensities of the ROI across V79 cells; (j) fluorescence intensities of the ROI across HeLa cells.

Highlights:

- ✓ The evaluation of equilibrium between phenoxazinium and phenoxazine skeletons indicated the deprotonated-protonated processes were under basic conditions.
- ✓ Comparative study of the influence of nitrophenyl and pyridinyl groups.
- ✓ One of the compounds shows the ability of lysosome biomarker.